DOI: 10.1002/adem.((please add manuscript number))

Glass Microparticles versus Microspheres-Filled Experimental Dental Adhesives**

By *Ensanya A. Abou Neel[1,2,3*], Azadeh Kiani[3], Sabeel P Valappil[4], Nicky M. Mordan[3], Song-Yi Baek[3], Kazi M. Zakir Hossain[5], Reda M. Felfel[6,7], Ifty Ahmed[6], Kamini Divakarl[8], Wojciech Chrzanowski[8], Jonathan C. Knowles[3,9,10]*

[*] *Prof. Ensanya A. Abou Neel Corresponding-Author & Author – One*

[1]Division of Biomaterials, Restorative Dentistry Department, King Abdualziz University, Jeddah, Saudi Arabia, [2]Biomaterials Department, Faculty of Dentistry, Tanta University, Tanta, Egypt, [3]UCL, Eastman Dental Institute, Biomaterials and Tissue Engineering Division, 256 Gray's Inn Road, London, WC1X 8LD.

E-mail: eabouneel@kau.edu.sa; e.abouneel@ucl.ac.uk

Dr. Azadeh Kiani – Author- Two

[3]UCL, Eastman Dental Institute, Biomaterials and Tissue Engineering Division, 256 Gray's Inn Road, London, WC1X 8LD.

E-mail: az_kiany@yahoo.com

Dr. Sabeel P Valappil– Author- Three

[4]Department of Health Services Research and School of Dentistry, University of Liverpool, Research Wing, Daulby Street, Liverpool, L69 3GN (UK)

E-mail: s.valappil@liverpool.ac.uk

Dr. Nicky M. Mordan – Author- Four

[3]UCL, Eastman Dental Institute, Biomaterials and Tissue Engineering Division, 256 Gray's Inn Road, London, WC1X 8LD.

E-mail: n.mordan@ucl.ac.uk

Dr. Song-Yi Baek - Author- Five

[3]UCL, Eastman Dental Institute, Biomaterials and Tissue Engineering Division, 256 Gray's Inn Road, London, WC1X 8LD.

Dr. Kazi M. Zakir Hossain

[5]Department of Chemistry, University of Bath, Claverton Down, Bath BA2 7AY, UK.

E-mail: z.hossain@bath.ac.uk

Dr. Reda M. Felfel – Author-Six

[6]Advanced Materials Research Group, Faculty of Engineering, University of Nottingham, UK. [7]Physics Department, Faculty of Science, Mansoura University, Mansoura 35516, Egypt.

E-mail: reda.felfel@nottingham.ac.uk

Dr. Ifty Ahmed– Author-Seven

[6]Advanced Materials Research Group, Faculty of Engineering, University of Nottingham, UK.

E-mail: ifty.ahmed@nottingham.ac.uk

Dr. Kamini Divakarla– Author-Eight

[8]The Australian Institute for Nanoscale Science and Technology The University of Sydney, NSW 2006, Sydney, Australia.

E-mail: skdivakarla@gmail.com

Dr. Wojciech Chrzanowski– Author-Nine

[8]The Australian Institute for Nanoscale Science and Technology The University of Sydney, NSW 2006, Sydney, Australia.

E-mail: wojciech.chrzanowski@sydney.edu.au

Prof. Jonathan C. Knowles– Author-Ten

[3]UCL, Eastman Dental Institute, Biomaterials and Tissue Engineering Division, 256 Gray's Inn Road, London, WC1X 8LD. [9]The Discoveries Centre for Regenerative and Precision Medicine, UCL Campus, London, UK, [10]Department of Nanobiomedical Science & BK21 PLUS NBM Global Research Center for Regenerative Medicine, Dankook University, Cheonan 31114, Republic of Korea. [11]UCL Eastman-Korea Dental Medicine Innovation Centre, Dankook University, Cheonan 31114, Republic of Korea

E-mail: j.knowles@ucl.ac.uk

[**] *Acknowledgements, general annotations, funding ((Supporting Information is available online from Wiley InterScience or from the author)).*

Abstract

This study aimed to formulate antibacterial dental adhesives. Phosphate-substituted methacrylate adhesives were modified with 0-20 wt% copper-doped glass microparticles. Two shapes of microparticles were used: regular-shaped (microspheres) and irregular-shaped (microparticles). The morphology/composition, roughness, monomer conversion (DC%), thermo-gravimetric analysis and antibacterial action against S. mutans and P. aeruginosa and ion release were investigated. The results showed that microspheres produced adhesives with a relatively smoother surface than microparticles. The DC% of adhesives increased with

increasing glass filler content. Filled adhesives showed polymer decomposition at ~315 °C and glass melting at 600 – 1000 °C. The weight loss% of adhesives decreased with increasing the wt% of fillers. 0-20 wt% glass microparticles significantly increased the antibacterial action of adhesives against both bacteria. 0-5 wt% glass microspheres significantly increased the antibacterial action of adhesives against both bacteria. Only 20 wt% microparticles-filled adhesive showed a similar inhibition zone to Tobramycin (positive control). Microparticle-filled adhesives (with >5 wt% filler) significantly reduced S. mutans than their microsphere counterparts. Microsphere-filled adhesives (with ≤5 wt% filler) significantly reduced P. aeruginosa than their microparticle counterparts. Microspheres-filled adhesives showed higher Cu release than their microparticles counterparts. Accordingly, phosphate-substituted methacrylate filled with glass could be used as antibacterial adhesives.

1. Introduction

Failure of dental restorations is usually caused by micro- [1] or nanoleakage [2] at the restoration-tooth interface. The need for a biological seal at the tooth-restoration interface is therefore a priority. Since the adhesive is the weakest link in dental restorations [3], its modification to remineralize defective dentin could play a major role in the success of dental restorations.

To produce a biological seal, several attempts have been done to incorporate antibacterial agents into dental adhesives. These agents include dimethylaminododecyl methacrylate (DMADDM) [4], quaternary ammonium salt [5] and chlorhexidine [6]. Most of these, however, can bind to dental adhesives (eg, DMADDM) and thus, their release can be limited. On the other hand, a significant release over a short period of time could occur with other agents (eg, chlorhexidine). In such cases, a reduction in mechanical properties will be expected. The need for an antibacterial agent that shows a long sustained release will, therefore, be of significance.

Bioactive phosphate-based glasses found great interest as fillers in composites for potential dental applications [7, 8]. They are degradable. Their degradation can be easily controlled to vary from hours to years according to their composition [9]. They release ions e.g. calcium and phosphate [8] that could potentially help in tooth remineralization. They can be doped with various oxides to impart different properties. For example, antibacterial actions can be introduced into these glasses by incorporation of oxides such as silver [10], copper [11] and zinc [12]. They can be prepared into different forms e.g., regular-shaped particles (microspheres) [13, 14] and irregular-shaped particles (microparticles). Unlike irregularly shaped particles, microspheres have a uniform shape and size. They, therefore, could improve the stiffness, impact resistance and surface finish of composites [13]. They also provide a comparatively larger surface area required for therapeutic coatings and ion release [13].

This study aimed to incorporate different wt% of copper-doped phosphate glass microparticles or microspheres into an experimental hydrophilic, phosphate-substituted methacrylate adhesive [15] – **See Figure 1**. The action of glass fillers on morphology, surface roughness, monomer conversion, thermal properties and antibacterial action of experimental adhesives was considered. The null-hypothesis was "there is no difference between glass-filled and unfilled adhesives regarding their morphology, the degree of monomer conversion, thermal properties and antibacterial action".

2. Experimental Section

2.1. Co-monomer

The experimental adhesive co-monomer used in this study is composed of 40 wt% 2,2-bis[4-(2-hydroxy-3-methyacryloyoxypropoxy)]-phenyl propane (BisGMA), 30% Bis-[2-(methacryloyloxy)ethyl] phosphate (BisMP), 28.75% 2-hydroxyethyl methacrylate (HEMA), 1% 2-ethyl-4-aminobenzoate (EDMAB) and 0.25% camphorquinone (CQ) [15] – **Table 1 (a)**.

2.2. Copper-Doped Phosphate Glasses

Copper-doped phosphate glasses, having the formula of $50P_2O_5$-30CaO-$10Na_2O$-10CuO, were prepared by melting an appropriate amount of NaH_2PO_4, $CaHPO_4$, P_2O_5 and CuO or $CuSO_4$ (Sigma-Aldrich, UK) – **Table 1 (b)**. The mix was melted at 1150 ^oC for 90 minutes using a 100 ml volume platinum-5% gold crucible. The crucible containing the precursors was first dried at 350^oC for 30 min prior to melting. The molten glass was then poured into a metal mould and allowed to cool down to room temperature to obtain the bulk glass.

The bulk glasses were ground into microparticles utilising a ball milling machine (Retsch PM100) and then sieved into size range of 30-125 μm. For the preparation of microspheres, the sieved microparticles were fed into the oxy-acetylene flame of a thermal spray gun (Metallisation Ltd, UK) using a hopper feeding system, as described elsewhere [16]. Post-manufacture, the microspheres were collected from the collection tube, washed with ethanol and dried overnight at 50 ^oC– **Figure 2 (a)**.

2.3. Experimental Adhesives

Glass microspheres or microparticles were added to the adhesive co-monomer at 0, 2.5, 5, 10 and 20 wt%. The resultant adhesives were coded as shown in **Table 2.** After mixing, the produced adhesives were then pressed between two acetate sheets to produce very thin films (~1 mm thick). Using the acetate sheets also exclude the atmospheric oxygen that could interfere with the polymerization reaction. Then curing was done using the visible light curing unit (Triad 2000, Dentsply, USA) for 120 s. The unit operated at 115 V-2.3 AMP and 50-60 Hz frequency – **Figure 2 (b)**.

2.4. Electron Microscopic Analysis/Energy Dispersive X-ray Microanalysis

The surface topography and cross-sectional morphology of unfilled and filled adhesives were characterised using scanning electron microscopy (SEM - Philips XL30, FEI, USA) at an accelerating voltage of 20 kV. A sputtered coating of Au was used to avoid image distortion due to charging.

The composition of glass microparticles and microspheres was analysed using energy dispersive X-ray micro-analysis (EDX) (Inca 400 EDX, Oxford Instruments Analytical, Abingdon, UK). Analysis was performed using a 20 kV beam and a large spot size. Samples were placed on carbon stickers and analysed. The weight and atomic percentage of each elements were used to calculate the mol% of CaO, CuO, P_2O_5 and Na_2O as given in the following equation.

$$Mol\ \% = \left(\frac{Weigth\%/Molar\ Mass\ of\ Oxide}{Total\ Mol}\right) x100$$

2.5. Nanomechanical Properties Mapping

Surface mapping of nanomechanical properties of samples (n=3) was investigated using PeakForce QNM (Multimode 8, Bruker, Santa Barbara) under tapping mode. Samples were mounted on magnetic holders fixed on the microscope stage. Samples were scanned using a silicon tip (RTESPA-300) with a spring constant of 40 $N.m^{-1}$ and frequency of 300 kHz. For each sample, at least three areas of 10×5 μm^2 were probed. The filler distribution and topography of each sample were obtained from the recorded maps.

2.6. Degree of Conversion (%)

The degree of co-monomer conversion (DC%) was measured using ATR-FTIR spectrometry (Perkin Elmer Series 2000, UK). FTIR of co-monomer and cured polymers were obtained at 37 °C after being centrally positioned on the Golden Gate Single Reflection Diamond ATR. Spectra at 500-4000 cm^{-1} were obtained using Timebase software with a resolution of 4 cm^{-1}. The degree of conversion (%) was calculated (n=3) from the following equation [17].

$$DC\% = \{1- [C_{aliphatic}/ C_{aromatic}] / [U_{aliphatic}/ U_{aromatic}]\} \times 100$$

Where $C_{aliphatic}$ and $C_{aromatic}$ are areas of absorption C=C peaks at 1637 and at 1608 cm^{-1} of the polymerized specimen respectively. Whereas $U_{aliphatic}$ and $U_{aromatic}$ are areas of absorption C=C peaks at 1637 and 1608 cm^{-1} of the unpolymerized specimen, respectively.

2.7. Thermal Analysis

Simultaneous differential scanning calorimetry (DSC) and thermogravimetric (TGA) analysis for the adhesives were conducted over 25-600 ºC using a TA Instruments SDT Q600. Thermal analysis was carried out under 100 mL min^{-1} nitrogen gas flow and 10 ºC min^{-1} heating rate. For the glass fillers, a higher temperature range (25-1000 °C) was used. For background correction, a blank run was conducted using an empty platinum pan. The heat flow and weight loss (%) of adhesives (~15 mg) were recorded against temperature. Data acquisition and processing were performed using TA Universal analysis 2000 software.

2.8. Agar Diffusion Assay

The antibacterial action of the experimental adhesives was tested against caries associated bacteria (*S. mutans* NCTC 10449) and opportunistic pathogen (*P. aeruginosa* ATCC27853) using disc diffusion assay [18]. The original stock of *S. mutans* or *P.aeruginosa* was maintained on brain heart infusion agar (BHI agar, Sigma-Aldrich, UK). *S. mutans* culture was carried out in an anaerobic environmental chamber [N_2:CO_2:H_2 = 80:10:10, Don Whitley MG1000; Don Whitley Scientific, Shipley, UK] at 37°C. *P.aeruginosa* culture was carried out in an aerobic environmental chamber at 37°C. Samples were incubated without shaking. The assay was repeated 3 times.

Cells of freshly grown overnight cultures of each bacteria were dispersed in phosphate buffered saline (Sigma -Aldrich, UK) to obtain a standardized culture of approximately 10^8 cells.ml^{-1}. A confluent layer of the standardized culture of each bacteria was spread on isosensitest agar (IST agar Oxoid, UK). Discs (n=3 & diameter = 5mm) of experimental adhesives along with positive

control discs were placed on agar. 50 µL of 0.2 % chlorhexidine digluconate (CHX, Oxoid, UK) and 225 ppm fluoride [F^-, FluoriGard, Colgate, UK] solution loaded onto a blank Oxoid™ Blank Antimicrobial Susceptibility Disks were used as positive controls for *S. mutans* experiment. Tobramycin (10µg, OxoidTM Basingstoke, UK) discs were used as positive controls for *P. aeruginosa* experiment. The diameters of any zones formed around the discs were measured in millimetres using a calliper.

2.9. Ion Release Measurements

A 5 x 4 mm2 sample from each experimental as well as unfilled adhesive was used for this study. Samples (n=3) for each adhesive were immersed in 20 mL deionised water (dH_2O) at 37 °C for 1, 5 and 7 days. Following each incubation, the samples were removed and transferred to a fresh 20 mL of dH_2O for further incubation. All effluent samples were stored at ≈ 4°C until required for analysis. Inductively Coupled Plasma – Optical Emission Spectroscopy (ICP-OES, (Varian 720-ES), machine was used in measuring the ion concentration. Two sets of identical calibration standard was prepared. This was done by diluting the ICP multielement standard solution with 5 % Nitic acid solution. The standard was run every 50 samples to make sure that the measurements were being done correctly.

2.10. Statistical Analysis

One-way analysis of variance (ANOVA) was used to test the significance difference between groups. The *t*-test was used was used to compare the mean of each series from microspheres-filled adhesives with its counterpart from microparticles-filled adhesives (eg, compare between 2.5CPMP and 2.5CSMP). The significance level was set at 0.5% and; SPSS 20 was used.

3. Results

3.1. Electron Microscopic Analysis

SEM images presented in **Figure 3 (a)** revealed the difference in morphology and size between glass microparticles and microspheres. The size of microspheres varies from 60-200 μm. The size of microparticles varied from <60-200 μm. It was difficult to accurately measure the lower range of size of microparticles due to their agglomeration. As given in **Table 3**, the elemental analysis of glass microparticles and microspheres showed that both forms have consistent results regarding the element atomic % and oxide mole %. However the P_2O_5 is much lower than expected. This in turn pushes up the other values as it is a percentage.

The top surface morphology of unfilled and filled adhesives are presented in **Figure 3 (b).** The unfilled adhesive exhibited a smooth blister-like surface texture. Microparticles-filled adhesives showed the dispersion of some microparticles on the top surface of samples. Microsphere-filled adhesives showed similar morphology to unfilled adhesives, but the blisters were comparatively larger and regular due to the presence of the microspheres.

Cross-sectional SEM images of unfilled adhesives also revealed a smooth surface (indicated by a green arrow). Microparticle-filled adhesives showed a comparatively rougher texture (indicated by yellow arrows). Microparticle-filled adhesives showed impregnation of microspheres within the polymer matrix (indicated by red arrows) - **Figure 3 (c).**

3.2. Nanomechanical Properties Mapping

As shown from **Figure 4,** the unfilled adhesive had a relatively smooth surface. Addition of 2.5 wt% of the glass microparticles produced localized sharp protrusions of few hundreds of nanometres to microns in size. Associated with these features, an increase in roughness was observed. The number of these features increased with increasing the filler content. With a microspherical glass filler, samples with 2.5 wt% filler showed the presence of a large number of smooth ‘wrinkle-like’ structures. The surface remained relatively smooth with filler content up to 5 wt%. A slight increase in roughness was only observed with samples containing >5 wt%

filler. This increase in roughness, however, was not statistically significant from the unfilled adhesive **- Table 2.**

3.3. Degree of Conversion (%)

Generally, the DC% was not adversely affected by the presence of glass fillers. Only high wt% of glass (>10 wt% microparticles or > 5 wt% microspheres) produced a significant increase in DC%. There were no significant differences in the degree of conversion of formulations filled with glass microspheres or microparticles. Only 5 and 10 wt% glass microspheres had a significantly higher degree of conversion than their microparticle-filled counterparts **- Table 2.**

3.4. Thermal Analysis

As seen from **Figure 5 (a)**, glass microspheres have a higher glass transition temperature (~410 °C) than microparticles (~395 °C). They also have an earlier crystallization peak (~570 °C) than microparticles (~605 °C). Only one melting peak was detected for microspheres (~715 °C), but two were seen for microparticles (700 and 720 °C). As seen from **Figure 5 (b)**, the unfilled adhesive has only one exothermic peak ascribed to polymer decomposition at ~315 ^{o}C. Filled adhesives have additionally a very broad melting peak (600 – 1000 ^{o}C) for glass microparticles or microspheres.

Upon heating the experimental adhesives, there is a significant weight loss that starts (25 – 270 °C) and ends (400 – 600 °C) gradually. Sharp weight loss was observed over 270 – 400 °C. The unfilled adhesive showed the maximum weight loss %. Increasing the amount of glass incorporated into the adhesive reduced the weight loss %– **Table 2**.

3.5. Agar Diffusion Assay

For antibacterial action against *S. mutans*, microparticles (up to 20 wt%) filled adhesives showed significantly larger inhibition zone than unfilled adhesives. Microspheres (only up to 5

wt%) filled adhesives showed significantly larger inhibition zones than unfilled adhesives. Regardless of this significant increase in antibacterial action, all experimental adhesives showed significantly smaller inhibition zone than positive controls (Chlorhexidine and fluoride). Regarding the glass powder shape and up to 5 wt%, there was no significant difference between microparticles and microspheres filled adhesives. Microparticles filled adhesives with > 5wt% showed a significantly larger inhibition zone than their microspheres counterparts – **Figure 6 (a & b).**

For antibacterial action against *P. aeruginosa*, all filled adhesives showed larger inhibition zones than unfilled adhesives. The only exception is the adhesive filled with 2.5 wt% microspheres that has similar inhibition zone to unfilled one – **Figure 6 (c & d).** Regardless of this significant increase in antibacterial action, all tested adhesives showed significantly smaller inhibition zone than positive controls (Tobramycin). The only exception is the adhesive filled with 20 wt% microparticles that has similar inhibition zone to the positive control. Regarding the glass powder shape, there was no significant difference between microparticles and microspheres filled adhesives at > 5 wt%. At ≤ 5 wt%, microspheres filled adhesives showed significantly larger inhibition zone than their microparticles counterparts – **Figure 6 (c & d).**

3.6. Ion Release Measurements

Regarding Ca release, the experimental adhesives showed Ca release but not the unfilled adhesive. Ca release increased with increasing the amount of glass fillers incorporated into the adhesive regardless of the glass form. It was increased with time. The microspheres filled adhesives showed higher release than microparticles filled counterparts. The highest release was detected for 20 wt% microspheres filled adhesives – **Figure 7 (a)**. Cu release showed similar trend to Ca – **Figure 7 (b).**

Regarding Na release, both unfilled and filled adhesives showed Na release; the higher release observed for the filled adhesives. No significant difference was observed between

microparticles and microspheres-filled adhesives – **Figure 7 (c).** Similar trend was also observed for P release – **Figure 7 (d).**

4. Discussion

Elimination of nanoleakage at the tooth-restoration interface is very challenging. Formulating an adhesive with both antibacterial (to inhibit the bacterial growth) and remineralizing actions (to strengthen the remaining tooth structure) would be the ultimate goal in dentistry.

In this study, both experimental adhesive monomer and glass fillers are hydrophilic. With water sorption, the release of ions (eg, calcium, phosphorous and copper) from the glass fillers would be expected. Calcium and phosphates would potentially help in re-mineralization of etched dentin particularly in those areas where the adhesive fails to penetrate. The copper, however, could help in caries prevention due to its antibacterial action. This study aimed to investigate the action of these glasses on surface roughness, the degree of monomer conversion, thermal and antibacterial properties of the experimental adhesive. The re-mineralizing potential of these experimental adhesives will be tested in the future.

Due to the hydrophilic nature of both experimental adhesive monomer and glass fillers, the possibility of filler agglomeration and subsequent phase separation upon their mixing was eliminated. The addition of glass microparticles or microspheres produced no significant change in surface roughness when compared with unfilled adhesives. Therefore, there is no reason to reject the null-hypothesis for surface roughness.

The degree of conversion is an important property in determining the effectiveness of the adhesive. A low degree of conversion results in low stiffness and hence low bond strength [19]. The addition of high weight % of microparticles or microspheres significantly enhanced the degree of conversion. This could indicate the proper dispersion of filler particles within the

polymeric matrix [20]. Maintaining the homogeneity of filled adhesives could therefore be responsible for the high degree of conversion obtained after the addition of fillers. When the size of the filler particles approaches the wavelength of the curing light, a scattering of light could occur. In such a case, a low degree of conversion will be expected. Since the size of glass filler particles is far from the wavelength of the curing light, the degree of conversion was not adversely affected in filled formulations [21]. The glass has got a halo shape absorbance band at 1640 cm^{-1} due to CuO. This band is very close to the polymer peak (1637 cm^{-1}). Then, CuO peak might be interfering with the 1637 cm^{-1} polymer peak, but not interacting with it as the 1637 cm^{-1} peak didn't show any shifting. CuO peak just reduced the absorbance intensity of the polymer peak (**See-S1)**. This could be accounted for the high degree of conversion obtained when high glass % where the intensity of CuO peak would be high. The degree of conversion of the unfilled adhesive is similar to that obtained by Carneiro et al., [22]. It is, however, lower than that obtained by Ito et al., [17]. This could be attributed to variation in the source and intensity of light curing. Therefore, the null hypothesis for DC% can be rejected.

The glass transition temperatures represent the point at which a large-scale molecular motion (primary or α-relaxation) will occur. Below the glass transition temperature, localized molecular motion (i.e., secondary or β-relaxations) can be expected. At higher temperatures, however, the flow of chains will occur. Therefore, the glass transition of any material used intra-orally should be higher than the mouth temperature [23]. The average glass transition temperature of the glass filler is ~400 °C. The differences in glass transition, crystallisation and melting temperature between microparticles and microspheres could be attributed to the differences in thermal history and the particle size. Teixeira and Rincon [24] found that crystallisation temperatures of SiO_2-CaO-Na_2O glass shifted to lower temperatures as the particle size decreased. They also reported that the height of crystallisation peak would increase as the particle size deceased. The microparticles were produced by grinding the melt-quenched

glass. The microspheres, however, were obtained by flame spheroidization which involves high temperatures. The surface area of microparticles is different from microspheres. The double melting peaks of microparticles could be due to the small size of particles [24]. Changing the thermal history and the particle size has no influence on the glass composition. As confirmed by EDX analysis, both glass microparticles and microspheres have similar composition. The Mole % of P_2O_5 however was lower than the actual one. This in turn pushes up the values of other oxides since all of them are presented as a percentage. This is not surprising as it is more likely to lose some P_2O_5 during glass preparation due to its volatile nature. Recently it has been shown by Gupta et al. [1] that the surface chemistry of the flame spheroidised phosphate-based glass microspheres of a particular size range (above 45 µm) didn't show significant differences in their chemical compositions compared to microparticles. However, the smaller microspheres (< 45 µm in diameter) produced from the same composition of microparticles revealed some compositional differences due to the migration of the lighter elemental oxides towards the surface due to their higher volatility. In this study, the microspheres utilised in the adhesive films were in the size range of 60-200 µm, therefore, negligible change in their surface chemistry during the flame spheroidization process was likely. The presence of carbon from polymer carbonization might be responsible for broadening of the melting peak of the glass seen at 600-1000 ºC. Addition of glass filler also reduced the weight loss %. This is expected due to the reduction in wt% of the polymer. The first stage of weight loss could be related to loss of residual ethanol and low molecular weight monomers eg, HEMA [19]. The second and third stage could be attributed to the decomposition of high molecular weight polymers [BisMP and BisGMA respectively] [19].

For the antibacterial study, *S. mutans* and *P. aeruginosa* were used. *S. mutans* is a gram-positive cocci and associated with caries [25]. *P. aeruginosa* is a gram-negative, rod-shaped, opportunistic multi-drug resistant bacteria. It is associated with root canal infection [26] and

biofilm formation [27]. The antibacterial action of the experimental adhesive could be related to the acidic nature of co-monomers used. Addition of glass fillers significantly enhanced the antibacterial action. This could be related to the release of Cu from experimental adhesives as shown from ion release data. The inhibitory action of copper was observed at a concentration of 0.16 microM against *S mutans* [28] and 0.1–0.8mg.L^{-1} against *P. aeurogenosa* [29]. Although copper is vital as a cofactor of many enzymes, it could be toxic to bacteria via metal catalysed protein oxidation and generation of reactive oxygen species [30]. The antibacterial action of 10 and 20 wt% microspheres-containing formulations showed no significant difference compared to the control adhesive. This could indicate that the level of copper release may be beyond the minimal inhibitory concentration. As observed from ion release data, the level of Cu release from both 10 and 20 wt% microspheres-containing formulations was 5.4±1.2 and 11.2±1.4 ppm (i.e, beyond the minimal inhibitory concentration). The variation seen between microsphere and microparticle filled adhesives could be related to the level of copper ion release. as As shown from Cu release data, microspheres filled adhesives showed significantly higher Cu release after 1 day than microparticles filled adhesives. . Generally, the null-hypothesis for antibacterial action will be rejected.

Characterization of these experimental adhesives in term of mechanical properties and adhesion to dentin will be considered in future work. The changes in mechanical properties that could occur over time and the glass filler could affect the penetration of adhesives into dentin will be also considered. The comparison will be carried out relative to commercially available adhesives as controls.

5. Conclusions

Incorporation of glass fillers (microparticles or microspheres) produced no significant change in surface roughness or DC%. Only high wt% of fillers produced a significant increase in DC%. Increasing the wt% of filler reduced the percentage weight loss. Furthermore, incorporation of

glass fillers (up to 5 wt%) significantly increased the antibacterial action of adhesives against *S. mutans* and *P. aeruginosa*. All tested filled adhesives, however, showed significantly smaller inhibition zone than the positive controls. The only exception is 20CPMP that showed similar inhibition zone to Tobramycin. Microparticles-filled adhesives (with >5 wt% filler) significantly reduced S. mutans than microspheres counterparts. Microspheres-filled adhesives (with ≤5 wt% filler) significantly reduced P. aeruginosa than microparticles counterparts. Generally, microspheres filled adhesives showed higher Cu release than their microparticles filled counterparts. The level of Cu release increased with increasing the glass filler content and incubation time.

Acknowledgement

The authors would like to highly acknowledge Professor David Pashly, Department of Oral Biology & Maxillofacial Pathology, School of Dentistry, Medical College of Georgia, Augusta, GA 30912-1129, USA, for kindly providing the co-monomer used in this study. The authors would also like to acknowledge the "Advanced Technology Dental Research Laboratory" at King Abdulaziz University, Faculty of Dentistry, Saudi Arabia.

Conflict of Interest

The authors declare that they have no conflict of interest regarding the materials discussed in this manuscript.

References

1. Carvalho AA, Moreira FCL, Cunha LM, Moura SMd, Souza JBd, Estrela C, et al. Marginal microleakage of class II composite resin restorations due to restorative techniques. Rev. odonto ciênc. **2010**;25(2):165-169.
2. Daifalla EML. Long-Term Nanoleakage Depth and Pattern of Cervical Restorations Bonded With Different Adhesives. Operative Dentistry, **2012**;37(1):45-53.
3. Paulette Spencer QY, Jonggu Park, Elizabeth M. Topp, Anil Misra, Orestes, Marangos YW, Brenda S. Bohaty, Viraj Singh, Fabio Sene, John Eslick, Kyle, Camarda aJLK. Adhesive/Dentin Interface: The Weak Link in the Composite Restoration. Ann Biomed Eng. **2010**;38(6):1989–2003.

4. Zhang K WS, Zhou X, Xu HH, Weir MD, Ge Y, Li M, Wang S, Li Y, Xu X, Zheng L, Cheng L. Effect of antibacterial dental adhesive on multispecies biofilms formation. J Dent Res. **2015**;94(4):622-629.
5. Li F CJ, Ma S, Zhang L, Xiao YH, Fang M. Antibacterial effects of a dental adhesive incorporating a quaternary ammonium monomer against Streptococcus mutans. Zhonghua Kou Qiang Yi Xue Za Zhi. **2009**;44(10):621-625.
6. Idris M. Mehdawi, Jonathan Prattena, David A. Spratt, Knowles JC, Young AM. High strength re-mineralizing, antibacterial dental composites with reactive calcium phosphates. Dental Materials **2013**;29:473–484.
7. P. B, K. G, C. KJ. Degradation properties and ion release characteristics of Resilon® and phosphate glass/polycaprolactone composites. International Endodontic Journal **2008**;41:1093-1100.
8. Prabhakar RL, Brocchini S, Knowles JC. Effect of glass composition on the degradation properties and ion release characteristics of phosphate glass—polycaprolactone composites. Biomaterials **2005**;26(15):2209-2218.
9. Abou Neel EA, Pickup DM, Valappil SP, Newport RJ, Knowles JC. Bioactive functional materials: a perspective on phosphate-based glasses. Journal of Materials Chemistry Review **2009**;Review (19):690-701.
10. Ahmed I, Abou Neel EA, Valappil SP, Nazhat SN, Pickup DM, Carta D, et al. The structure and properties of silver-doped phosphate-based glasses. Journal of Materials Science **2007**; 42 (23): 9827-9835.
11. Abou Neel EA, Ahmed I, Pratten J, Nazhata SN, Knowles JC. Characterisation of antibacterial copper releasing degradable phosphate glass fibres. Biomaterials **2005**;26:2247–2254.
12. Abou Neel EA, O'Dell LA, Smith ME, Knowles JC. Processing, characterisation, and biocompatibility of zinc modified metaphosphate based glasses for biomedical applications. Journal of Materials Science: Materials in Medicine **2008**;19 (4):1669-1679.
13. Kazi M. Zakir Hossain U, Ifty Ahmed. Development of microspheres for biomedical applications: a review. Progress in Biomaterials **2015**;4(1):1–19.
14. a NJL, J-HPb, c, NJMa, VSa, IBWb, d, H-WKb, c, et al. Titanium phosphate glass microspheres for bone tissue engineering. Acta Biomaterialia **2012**;8:4181–4190.
15. Y. Nishitani MY, A.M. Donnelly, K.A. Agee, J. Sword2, F.R. Tay, and D.H. Pashley. Effects of Resin Hydrophilicity on Dentin Bond Strength. 85 **2006**;J Dent Res(11):1016-1021.
16. K. M. Z. Hossain UP, A. R. Kennedy, L. Macri-Pellizzeri, V. Sottile, D. M. Grant, B. E. Scammell, I. Ahmed. Porous calcium phosphate glass microspheres for orthobiologic applications. Acta Biomaterialia **2018**;72:396-406.
17. Shuichi Ito MH, Bakul Wadgaonkar, Nadia Svizerod, Ricardo M. Carvalho, Cynthia Yiuf, Frederick A. Rueggebergg, Stephen Foulgerh, Takashi Saitoa,Yoshihiro Nishitanii, Masahiro Yoshiyamai, Franklin R. Tay, David H. Pashley,. Effects of resin hydrophilicity on water sorption and changes in modulus of elasticity. Biomaterials **2005**;26:6449–6459.
18. JM A. BSAC standardized disc susceptibility testing method (version 4). J Antimicrob Chemother **2005** 56(1):60-76.
19. Lívia Rodrigues de Menezesa EOdS. The Use of Montmorillonite Clays as Reinforcing Fillers for Dental Adhesives. Materials Research **2016**;19(1):236-242.
20. T. G. Nunes, Pereira SG, Kalachandra S. Effect of treated filler loading on the photopolymerization inhibition and shrinkage of a dimethacrylate matrix. Journal of Materials Science: Materials in Medicine **2008**;19(5): 1881–1889.
21. Turssi CP, Ferracane JL, Vogel K. Filler features and their effects on wear and degree of conversion of particulate dental resin composites. Biomaterials **2005**;26(24):4932-4937.
22. Karina Kato Carneiro1 MMM, Clenilton Costa dos Santos3,, Adeilton Pereira Maciel4 CNC, José Bauer6. Adhesives Doped with Bioactive Niobophosphate Micro-Filler: D e g r e e

o f C o n v e r s i o n a n d Microtensile Bond Strength. Brazilian Dental Journal **2016**;27(6):705-711.
23. J.C.S. Moraes SaCRG. Materials Science » Composite Materials » "Metal, Ceramic and Polymeric Composites for Various Uses", Chapter 33: The Glass Transition Temperature in Dental Composites 2011.
24. Teixeira SR, Romero M, Rincón JM. Crystallization of SiO2–CaO–Na2O Glass Using Sugarcane Bagasse Ash as Silica Source. J. Am. Ceram. Soc. **2010**;93(2):450-455.
25. Forssten SD, Björklund M, Ouwehand AC. Streptococcus mutans, Caries and Simulation Models. Nutrients **2010**;2(3):290-298.
26. Ranta K HM, Ranta H. Monoinfection of root canal with Pseudomonas aeruginosa. Endod Dent Traumatol. **1988**;4(6):269-272.
27. Tsiry Rasamiravaka QL, Pierre Duez, Mondher El Jaziri. The Formation of Biofilms by Pseudomonas aeruginosa: A Review of the Natural and Synthetic Compounds Interfering with Control Mechanisms. BioMed Research International **2015**;2015:Article ID 759348, 759317 pages.
28. H Aranha RCS, J E Arceneaux and B R Byers. Effect of trace metals on growth of Streptococcus mutans in a teflon chemostat. . Infect. Immun. **1982** 35 (2):456-460.
29. Hsin-I Huanga H-YS, Chien-Ming Leeb,c, Thomas C. Yangb , Jiunn-Jyi Layd , Yusen E. Lina, . In vitro efficacy of copper and silver ions in eradicating Pseudomonas aeruginosa, Stenotrophomonas maltophilia and Acinetobacter baumannii: Implications for on-site disinfection for hospital infection control. Water Research **2008**;42:73-80.
30. Rensing CaG, G. . Escherichia colimechanisms of copper homeostasis in a changing environment. FEMS Microbiol Rev **2003**;27:197–213.

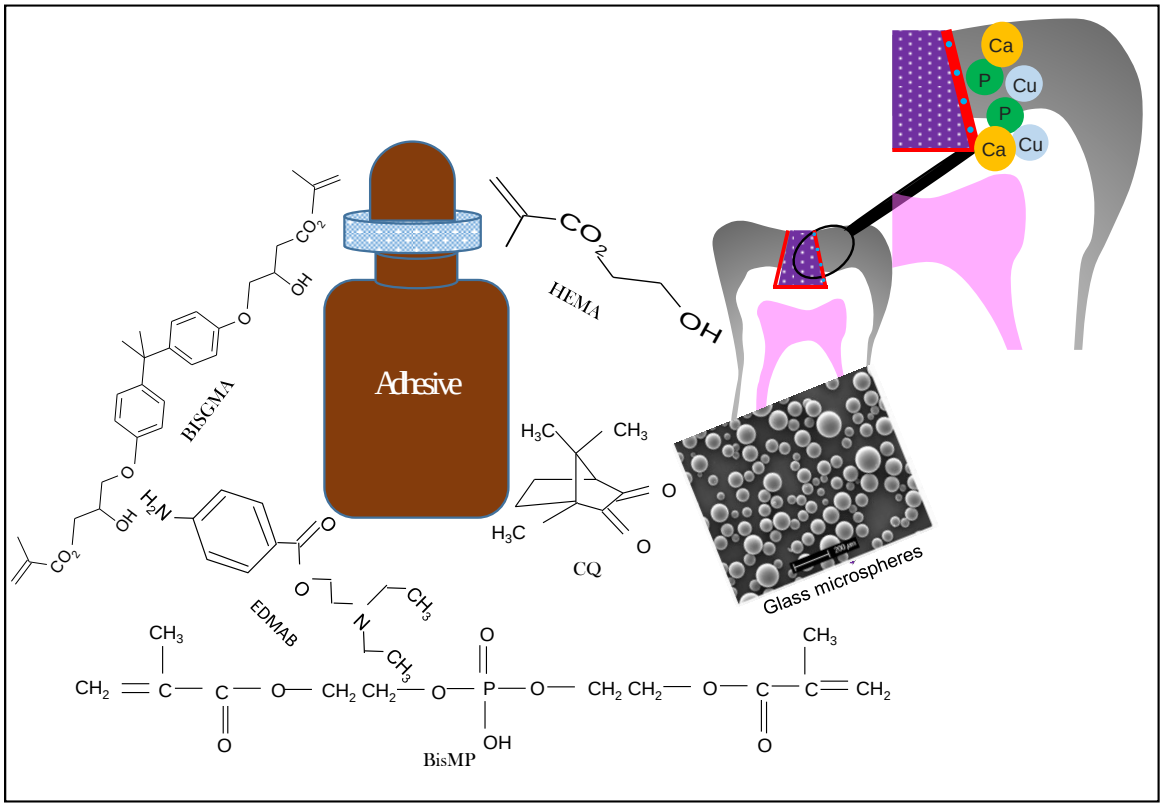

Figure 1: Diagrammatic representation of the experimental adhesives showing both monomer and glass microspheres components. The expected ion release involves Ca and P that will potentially be responsible for remineralization of tooth. Cu could provide antibacterial action at tooth-restoration interface.

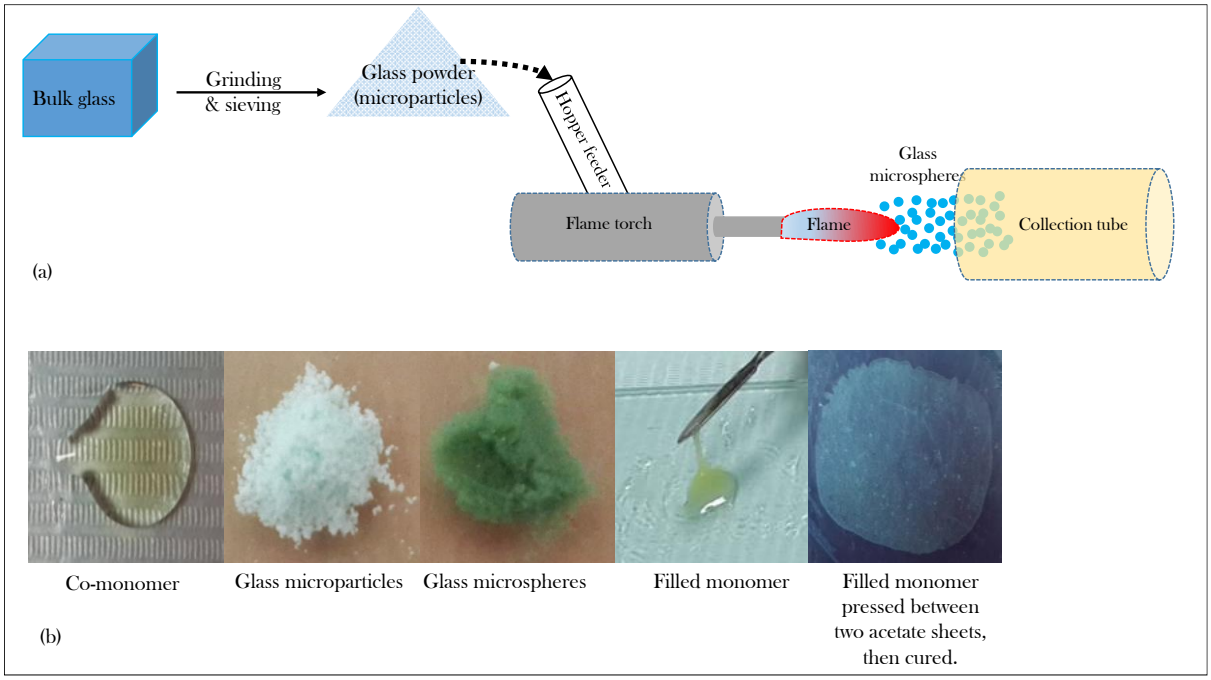

Figure 2: (a) Schematic representation of microspheres production using flame spheroidization method. (b) Steps of preparation of experimental adhesives films.

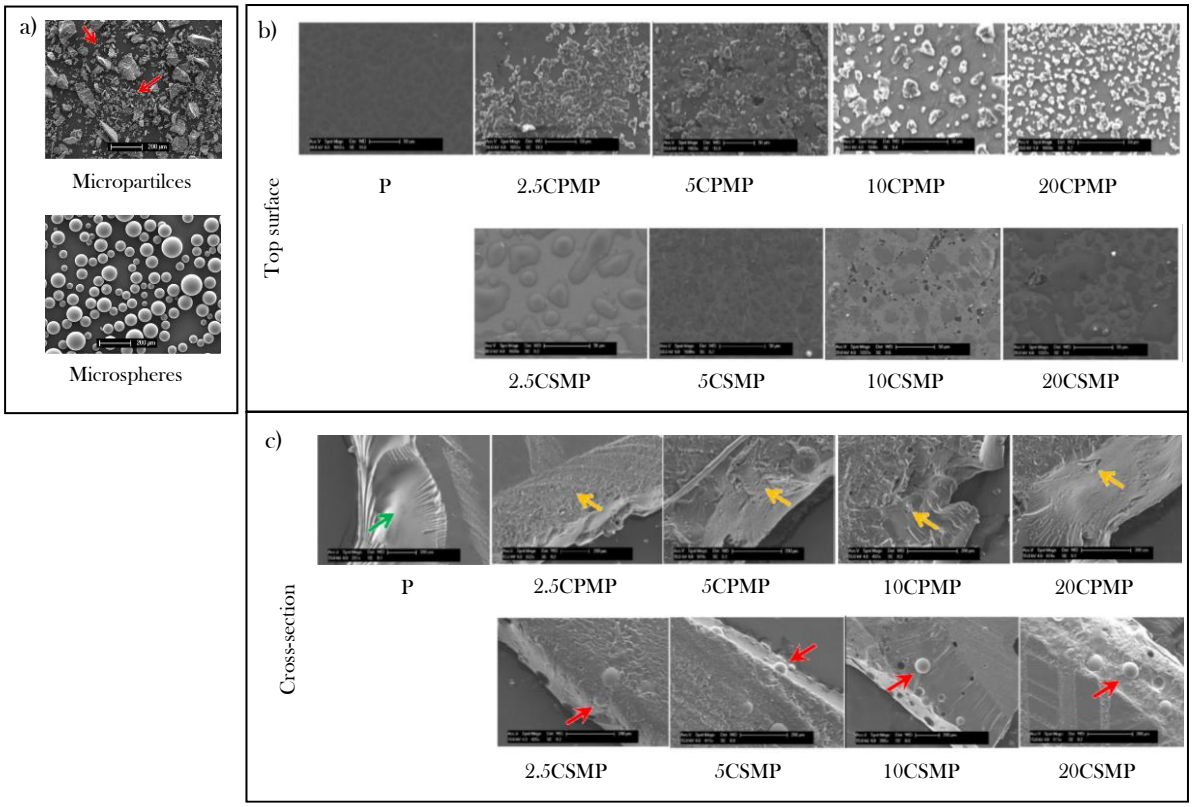

Figure 3: SEM images of: a) glass microparticles and microspheres. Microparticles have irregular morphology and slightly larger range of sizes than microspheres. Red arrows refer to some of the lower size range of particles (<60 µm). b) top surface of experimental adhesives produced using various weight % of glass microparticles and microspheres (scale bar 50 µm). Both unfilled adhesives and microspheres filled adhesives showed smooth blister-like surface texture. The blisters were comparatively larger and regular in filled than unfilled formulations. Microparticles filled adhesives showed the dispersion of some microparticles on the top surface. c) cross-section of experimental adhesives produced using various weight % of glass microparticles and microspheres (scale bar 200 µm). Impregnation of microspheres in the polymer matrix was observed.

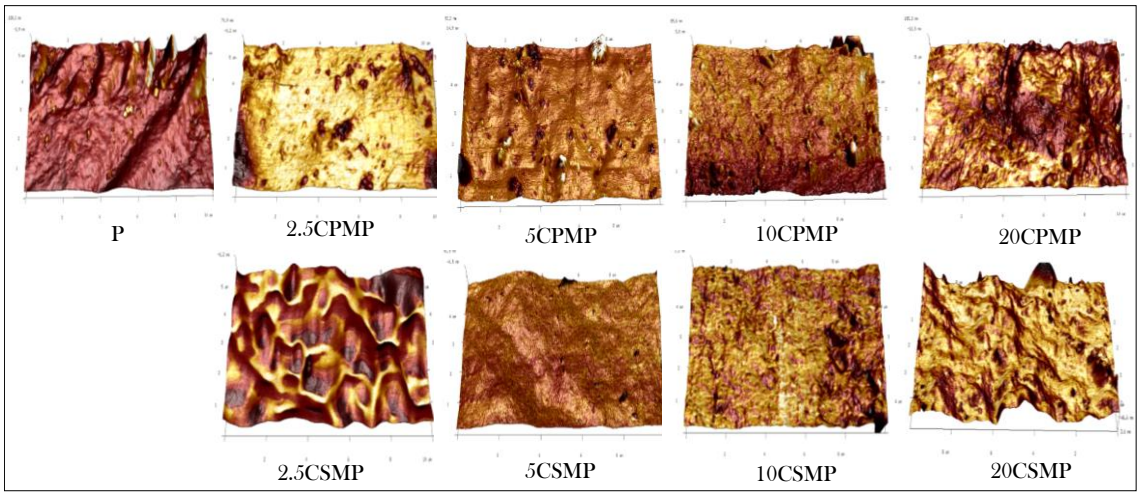

Figure 4: 3D images of the surface of tested formulations. The roughness increased with increasing the glass filler content.

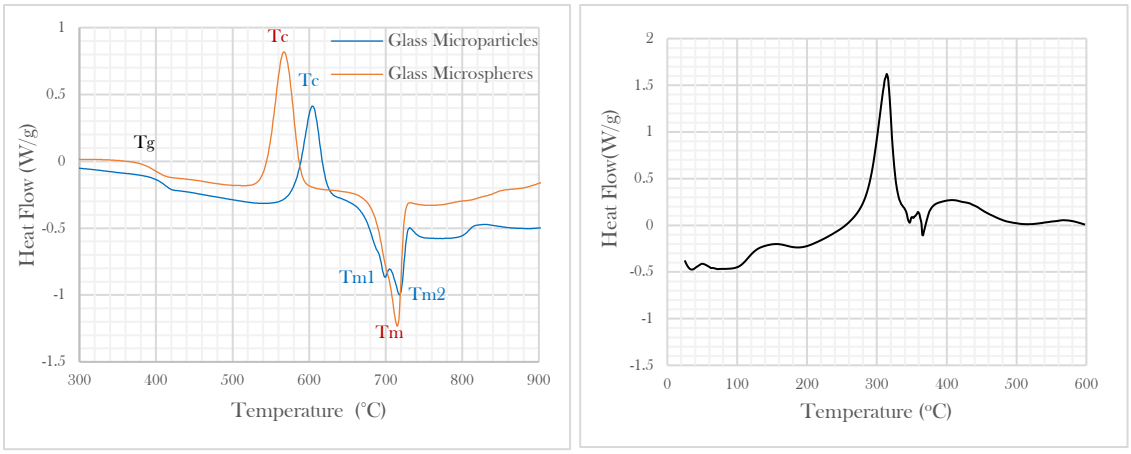

(a) (b)

Figure 5: Differential scanning thermogram of glass microparticles versus microspheres (a) and unfilled adhesive (b).

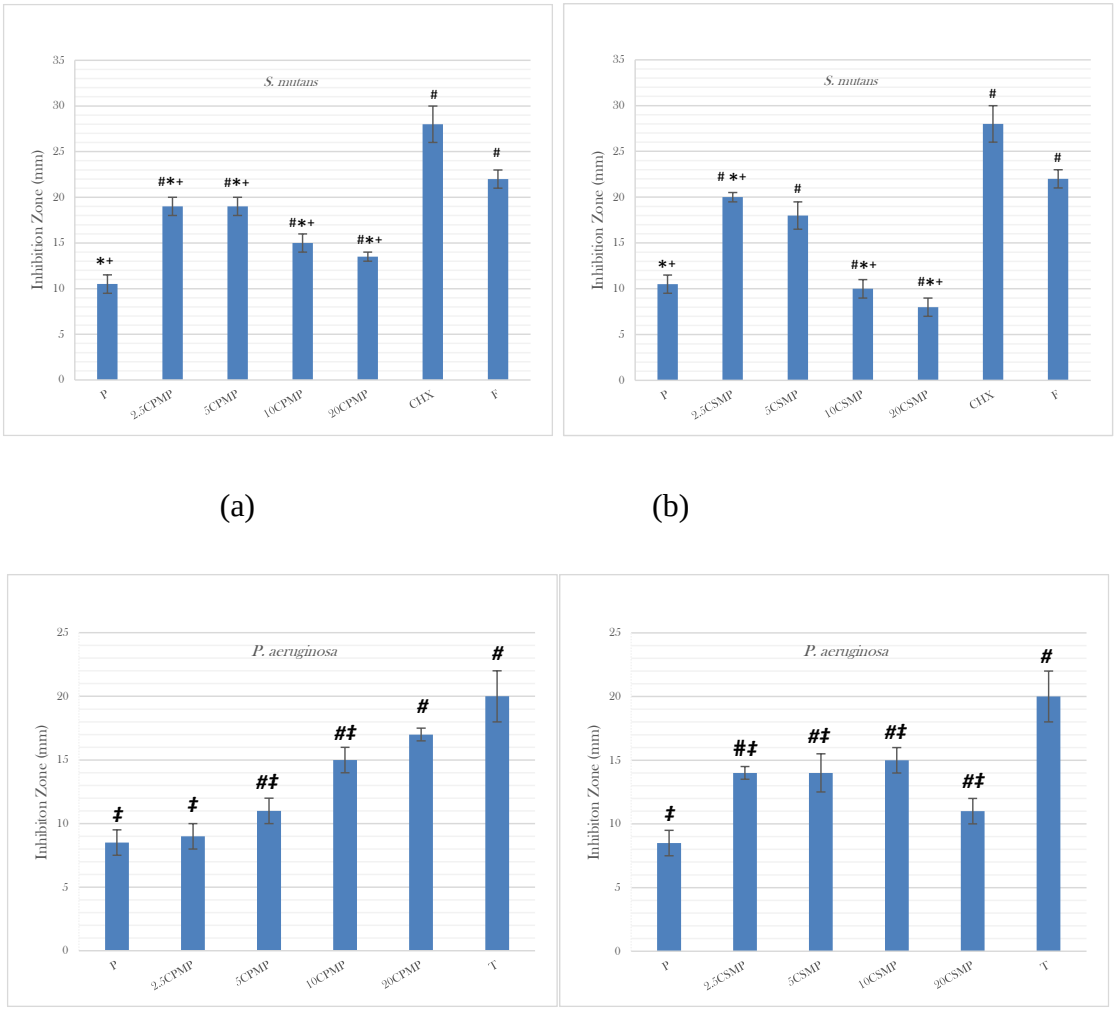

*Figure 6: Inhibition zone (mm) for S. mutans (a & b) and P. aeruginosa (c & d) for all tested adhesive formulations. CHX (chlorhexidine) and F (fluoride) were used as positive controls for S. mutans study. T (tobramycin) was the positive control for P. aeruginosa study. #, *, +, ‡ show a significant difference from unfilled adhesives, CHX, F and T respectively. The significant level was 0.05. For S. mutans, all filled formulations (except 10 & 20CSMP) showed significantly larger inhibition zone than unfilled adhesives. They however have smaller inhibition zone than fluoride and Chlorhexidine. For P. aeruginosa, all filled formulations (except 2.5 CPMP) showed larger inhibition zone than the unfilled adhesives. They (except 20CPMP) however have smaller inhibition zone than Tobramycin. For s. mutans, >5 wt% microparticles filled adhesives have significantly larger inhibition zone than microspheres filled counterparts. For p. aeruginosa, <5 wt% microsphere produced significantly larger inhibition zone than microparticles filled counterparts.*

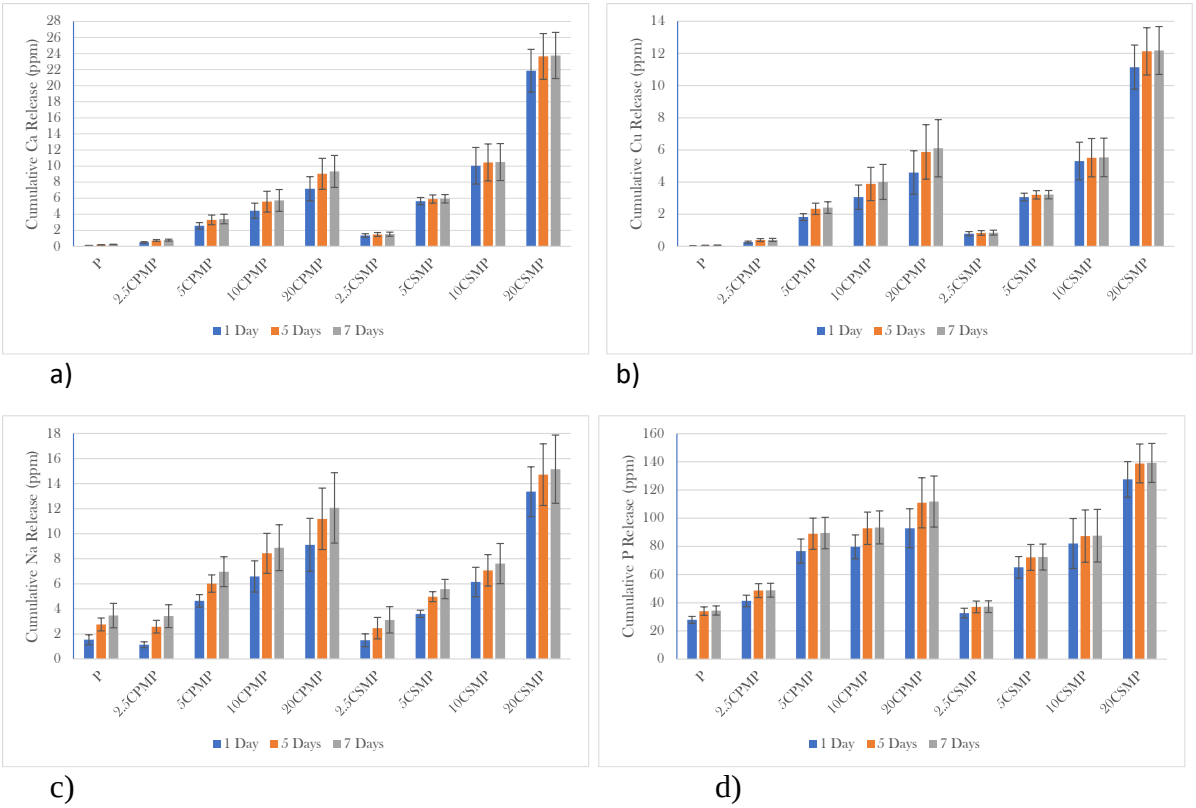

Figure 7: Cumulative ion release data: (a) Ca, (b) Cu, (c) Na and (d) P in ppm.

Table 1: (a) Composition of the co-monomer (Mol% and structure of each component) used to provide the matrix for the experimental adhesives. (B) Precursors used, oxides required for

preparation of glass microparticles and microspheres (the filler phase of the experimental adhesives) and mole% of each oxide.

(a) Co-monomer			
Component	**Abbreviation**	**Mol %**	**Structure**
2,2-bis[4-(2-hydroxy-3-methyacryloyoxypropoxy)]-phyenyl propane	BisGMA	19.6	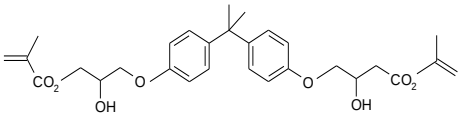
Bis-[2-(methacryloyloxy)ethyl] phosphate	BisMP	23.4	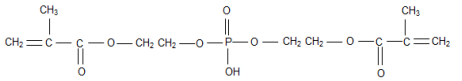
2-hydroxyethyl methacrylate	HEMA	55.5	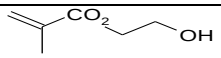
2-ethyl-4-aminobenzoate	EDMAB	1.2	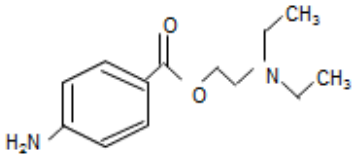
Campherquinone	CQ	0.4	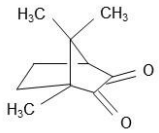
(b) Copper-doped phosphate glass microparticles or microspheres			
Precursors Used/Chemical Formula	**Oxides Required /Chemical Formula**	**Oxides Mole %**	
Phosphorous pentoxide/ P_2O_5	Phosphorous pentoxide /P_2O_5	50	
Calcium hydrogen phosphate/ $CaHPO_4$	Calcium oxide/CaO	30	
Sodium dihydrogen phosphate/NaH_2PO_4	Sodium oxide/Na_2O	10	
Copper sulphate ($CuSO_4$) for microparticls or Copper oxide/CuO for microspheres	Copper oxide/CuO	10	

*Table 2: Codes, filler wt%/filler form, description, roughness (RQ & Ra), degree of monomer conversion (DC %) and weight loss % of experimental adhesives used in this study. * refers to statistical significance difference from the control (P). Significance level 0.05.*

Codes	Filler wt%/Filler Form	Description	Roughness (nm)		DC%	Weight Loss %
			RQ	Ra		
P	0/NA	polymer (unfilled adhesive)	19.4 ± 4.6	15.2 ± 3.2	44.7 ± 2.9	69
2.5CPMP	2.5/microparticles	copper-glass microparticles modified adhesive	26.6 ± 8.2	19.1 ± 5.4	46.7 ± 2.7	66
5CPMP	5/ microparticles		27.9 ± 6.7	20.9 ± 4.7	41.5 ± 2.0	65
10CPMP	10/ microparticles		17.9 ± 6.5	14.1 ± 5.8	44.4 ± 2.1	64
20CPMP	20/ microparticles		19.6 ± 7.0	15.5 ± 5.8	57.0 ± 2.8*	60
2.5CSMP	2.5/microspheres	copper-glass microspheres modified adhesive	19.8 ± 6.6	15.5 ± 5.3	44.5 ± 3.1	65
5CSMP	5/ microspheres		17.0 ± 2.4	13.3 ± 1.7	49.5 ± 2.3	64
10CSMP	10/ microspheres		20.9 ± 10.1	16.6 ± 8	55.7 ± 2.9*	61
20CSMP	20/ microspheres		15.3 ± 1.2	11.2 ± 1.1	56.3 ± 3.0*	55

Table 3: Element (Atomic %) and oxid (Mole %) for both glass microparticles and microspheres as detected by EDA analysis.

	Elements (Atomic %)	Na	P	Ca	Cu
Microparticles	AVE.	14.6	63.3	17.0	5.1
	SD.	1.2	1.1	1.1	0.8
Microspheres	AVE.	13.7	64.7	16.8	4.8
	SD.	1.2	0.5	1.4	1.4
	Oxide (Mol %)	**Na_2O**	**P_2O_5**	**CaO**	**CuO**
Microparticles	AVE.	15.3	39.0	34.2	11.5
	SD.	1.4	1.3	1.8	1.7
Microspheres	AVE.	14.5	40.3	34.4	10.8
	SD.	1.5	1.1	2.6	3.2

Received: ((will be filled in by the editorial staff))
Revised: ((will be filled in by the editorial staff))
Published online: ((will be filled in by the editorial staff))

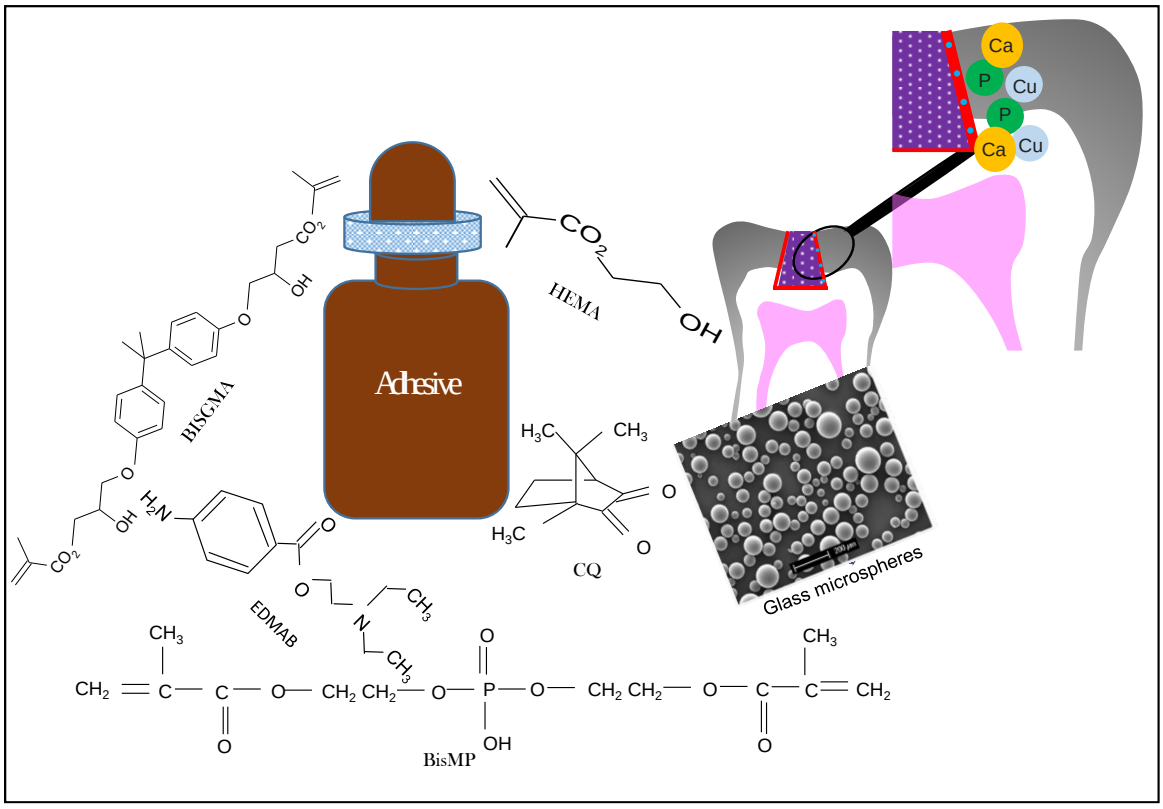

Diagrammatic representation of the experimental adhesives showing the monomer components used in the preparation as well as the glass microspheres. The expected ions release (eg, Ca and P that will potentially be involved in remineralization of tooth and Cu that could provide antibacterial action) at tooth-restoration interface.

Prof. Ensanya A. Abou Neel Corresponding-Author & Author – One, Dr. Azadeh Kiani – Author- Two, Dr. Sabeel P Valappil– Author- Three, Dr. Nicky M. Mordan – Author- Four, Dr. Kazi M. Zakir Hossain, Dr. Reda M. Felfel – Author-Five, Dr. Ifty Ahmed– Author-Six Dr. Kamini Divakarla– Author-Seven, Dr. Wojciech Chrzanowski– Author-Eight, Prof. Jonathan C. Knowles– Author-Nine

Glass Microparticles versus Microspheres-Filled Experimental Dental Adhesives

1. Gupta D, Hossain KMZ, Ahmed I, Sottile V, Grant DM. Flame-Spheroidized Phosphate-Based Glass Particles with Improved Characteristics for Applications in Mesenchymal Stem Cell Culture Therapy and Tissue Engineering. ACS applied materials & interfaces **2018**;10(31):25972-25982.